Pharm Res (2010) 27:2394–2401
DOI 10.1007/s11095-010-0175-x

RESEARCH PAPER

Nanocomposite Formulation System of Lipid-Regulating Drugs Based on Layered Double Hydroxide: Synthesis, Characterization and Drug Release Properties

Mohamed R. Berber • Inas H. Hafez • Keiji Minagawa • Takeshi Mori • Masami Tanaka

Received: 1 April 2010 / Accepted: 17 May 2010 / Published online: 29 May 2010

ABSTRACT

Purpose To design a nanocomposite formulation system of lipid-regulating drugs with versatile approaches using layered double hydroxide (LDH) material.

Methods The co-precipitation technique has been used to prepare the selected drugs [bezafibrate (BZF) and clofibric acid (CF)]-LDH nanocomposites. The nanocomposite materials (BZF-LDH and CF-LDH) were characterized by X-ray powder diffraction, infrared spectroscopy, thermogravimetric analysis, and scanning electron microscopy. The *in vitro* study was investigated in simulated gastrointestinal solutions at 36.8°C.

Results X-ray measurement and spectroscopic analysis indicated the formation of fully monophase drug-nanocomposites. The nanocomposites' gallery heights were calculated to be 23.5 and 16.3Å for BZF and CF, respectively. The new gallery heights indicated that BZF and CF drugs have been stacked into LDH as a monolayer with a staggered inter-digitated arrangement. The size of the nanocomposites described by SEM microscopy was~0.1 μm. The nanocomposite formulation has improved the drugs properties (thermal stability, dissolution, and controlled release) beside the achievement of drug target delivery.

Conclusions Nanocomposites composed of lipid-regulating drugs (BZF and CF) with LDH were successfully synthesized as a new formulation system of this drug category. The LDH nanocomposite formulation system has improved the drugs release properties.

KEY WORDS fibrates · LDH · nanocomposites · formulations · controlled delivery

INTRODUCTION

Coronary heart disease is associated with the elevation of serum lipid concentrations (cholesterol and triglycerides) resulting from smoking and some genetic disorders (1,2). In such disease cases, to reach the normal blood lipid target ratios, treatment with hypolipidemic drugs is required. Fibrates such as bezafibrate (BZF) and clofibric acid (CF) are a class of lipid-regulating drugs that have been used in the therapy in many forms of hyperlipoproteinemia (3). BZF (2-[4-(2-[4-chlorobenzamindo] ethyl)-phenoxy]-2-methyl-propanoic acid) is a well-known antihyperlipidaemic agent that lowers elevated blood serum lipid concentrations (cholesterol and triglycerides) (4). CF [2-(4-Chloro phenoxy)-2-methylpropanoic acid] is the active metabolite of the blood lipid regulator colfibrate. It lowers elevated serum lipids by reducing the very low-density lipoprotein fraction that is rich in triglycerides (5). Usually fibrates are administrated orally. Their maximal adsorptions mainly take place in the duodenum and the small intestine of the gastrointestinal tract (6). However, fibrates

M. R. Berber · I. H. Hafez · K. Minagawa
Institute of Technology and Science, The University of Tokushima
Tokushima 770-8506, Japan

T. Mori
Department of Applied Chemistry, Kyushu University
Fukuoka 819-0395, Japan

M. Tanaka
Faculty of Pharmaceutical Sciences, Tokushima Bunri University
Tokushima 770-8514, Japan

M. R. Berber (✉) · K. Minagawa (✉)
Department of Chemical Science, and Technology,
Institute of Technology and Science, The University of Tokushima,
Tokushima 770-8506, Japan
e-mail: mrberber@sy34.chem.tokushima-u.ac.jp
e-mail: minagawa@chem.tokushima-u.ac.jp

have poor water solubility (3), are sensitive to light and oxidation (especially CF) (7), and contain a carboxylic acid group that can impart local gastrointestinal irritation. Thus, significant oral bioavailability of fibrates can be problematic.

Fibrate products currently available on the market are based on conventional formulations (milling, micronization and microcoating) (8–10). These formulations are raising only the drug surface area for rapid dissolution using complicated and technically challenging processes. The resultant micronized drug is usually comprised in capsules or tablets. Accordingly, there is a high tendency for fibrates to recrystallize, and this may reduce the bioavailability. Driven by the mentioned administration problems of fibrates and the demand of constant levels of blood lipids to avoid the disorders of the cardiovascular system, more developed formulations of fibrates with controlled delivery doses are needed. An innovative approach to oral drug delivery in the small intestine involves the use of nano-fabricated delivery systems. This platform offers potential advantages over the traditional oral drug delivery approaches.

Layered double hydroxide (LDH) is natural clay that can be prepared by co-precipitation of M^{2+} and M^{3+} metal ions (*e.g.* Mg^{2+} and Al^{3+}). It consists of layers of edge-sharing hydroxyl octahedral with net positive charge balanced by anions in the interlayer (11,12). LDH has hosting properties to create nanocomposite structures. Many kinds of beneficial organic anions have been stacked as guests into the interlayer of LDH, such as drugs, vitamins and nucleic acids. Drug-LDH nanohybrid materials have been formulated to control drug release properties, drug solubility and dissolution (13–17). In addition, the amount of the incorporated drug into LDH has been controlled by changing the composite preparation technique (17). The intercalation of vitamins (18) and nucleic acids (19) into LDH offered a safe preservation of the guest bioactivity without any deterioration of the structural integrity. In addition, LDH has anti-acid and anti-pepsin properties (20) that can serve in the decrease of gastrointestinal irritation resulting from oral administration of drugs containing carboxylic acid groups. These interesting properties of LDH are expected to be advantageous for fibrates' low solubility, preservation and controlled release properties.

Based on our knowledge, there is no report concerning the target delivery and the control release properties of lipid-regulating drugs (fibrates) in a form of nanocomposite. Here, we report the synthesis and characterization of fibrate (BZF and CF) nanocomposites with LDH as a new formulation system of this drug category, as well as release studies to evaluate the effect of LDH on the drug properties after the intercalation process.

MATERIALS AND METHODS

Materials

Magnesium chloride hexahydrate, aluminum chloride hexahydrate, (Kanto Chemical Co., Inc.), Bezafibrate drug (Sigma, purity≥98 %) and clofibric acid drug (Sigma, purity 97 %) were used without further purification.

Nanocomposites Synthesis by Co-precipitation Technique

Co-precipitation technique (17) has been used to synthesize the nanocomposite materials of the selected drugs with a good loading ratio as follows: BZF drug (1 g) was dissolved in 60 ml deionized water by adjusting the solution pH at 8 using 2 M KOH. To the drug solution, 30 ml aqueous solution containing 1.23 g $MgCl_2{\cdot}6H_2O$ and 0.73 g $AlCl_3{\cdot}6H_2O$ (M^{2+}/M^{3+} molar ratio = 2) was added dropwise with stirring. During the addition, the pH of the suspension was kept constant at 8 by adding appropriate amounts of 2 M KOH solution. The final volume was augmented to 100 ml by deionized water. The suspension was stirred at 70°C for 24 h under N_2 flow. After the reaction, the obtained BZF-LDH material was collected by filtration (0.45-μm Millipore membrane), washed several times with 0.1 M KOH and deionized water, and finally freeze dried. By the same procedure, CF-LDH and LDH (reference) were prepared. For LDH preparation, potassium carbonate has been used instead of the drug.

Drug Content Determination

The amount of drug loaded into LDH was calculated using UV quantitative method. A known amount of the nanocomposite was dissolved in 10 ml of 1 M HCl, then the obtained solution was diluted with phosphate buffer (pH 7.4). The drug concentration was determined by UV absorption at 229 and 224 nm for BZF and CF, respectively. The drug content was expressed by the percentage of drug weight intercalated in a unit weight of nanocomposite. The UV quantitative method was also used to check the drug integrity before and after intercalation process.

Drug Delivery and Release Measurements

The dissolution of the original drugs (BZF, CF) and their nanocomposites (BZF-LDH, CF-LDH) were monitored in the following buffer mediums: buffer A as a simulated stomach solution (0.1 M HCl / 0.1 M KCl, pH 2.0), buffer B as a simulated duodenum solution (100 ml solution of 0.1 M $NaHCO_3$ / 0.1 g NaCl / 0.05 M HCl to adjust pH

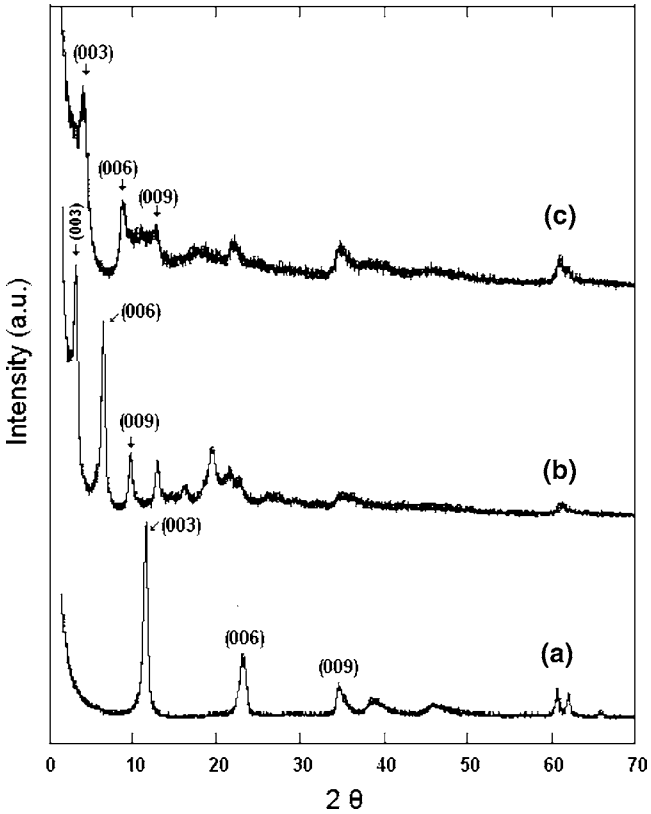

Fig. 1 X-ray diffraction patterns of LDH (**a**), BZF-LDH (**b**) and CF-LDH (**c**).

at 6.0) and buffer C as a simulated small intestine solution (100 ml solution of 0.1 M $NaHCO_3$ / 0.1 g NaCl / 0.05 M HCl to adjust pH at 8.0). The anionic buffer composition was defined based on literature data (21,22). Taking into account both of the usual daily dose of the selected drugs (~ 400 mg/day) (6) and the drug loading ratio into LDH (as described in Results and Discussion section), the release experiments were conducted with sufficient amounts of the intercalated drugs-LDH materials to study the effect of LDH on the drug-release properties and to ensure a good therapeutic effect. Accordingly, the release experiment was performed as follows: In a round-bottom flask, a sample of 200 mg (in the case of nanocomposite) or 100 mg (in the case of drug powder, taking into account the drug loading ratio) was dispersed in 100 ml buffer which was maintained at 36.8±0.1°C with a constant agitation of 80 round/min. At appropriate time intervals, 1.0 ml sample was withdrawn and filtered using a 0.45-μm Millipore filter unit to remove the insoluble particles. The filtrate was diluted and assayed with a UV spectrophotometer (U-3210, Hitachi, Japan) at λmax of 229 and 224 nm for BZF and CF, respectively. The removed aliquot was immediately replenished with the same volume of buffer equilibrated at the same temperature. The dissolution experiment of each sample was performed in duplicates.

Characterization

X-ray powder diffraction patterns were recorded on Rigaku X-ray diffractometer using Cu*K*α radiation at λ =1.5405 Å. The measurement was performed in the 2θ range 1.5–70° with a 2θ scanning step 0.02°, scanning step time 5 s, a filament intensity 40 mA and a voltage of 150 kV. Infrared spectra (KBr disk method) were recorded on a BioRad-FTS 3000MX FT-IR spectrophotometer with a TGS detector in the wavenumber range 4000–450 cm^{-1} by accumulating 16 scans at 4 cm^{-1} resolution. Thermogravimetric analysis (TGA) was conducted with Shimadzu thermogravimetric analyzer (TGA-50, TA-60WS) using platinum cell with a heating rate of 10°C / min under N_2 flow of 20 ml/min. The scanning electron micrographs (SEM) were captured by Hitachi FE-SEM S-4700 microscope.

RESULTS AND DISCUSSION

X-ray Powder Diffraction

Figure 1 shows the XRD patterns of the samples prepared by the co-precipitation technique. Pattern (a) indicated the formation of a single phase LDH with sharp and symmetric (*00l*) reflections. Using Bragg's law (nλ=2*d*sinθ), the basal

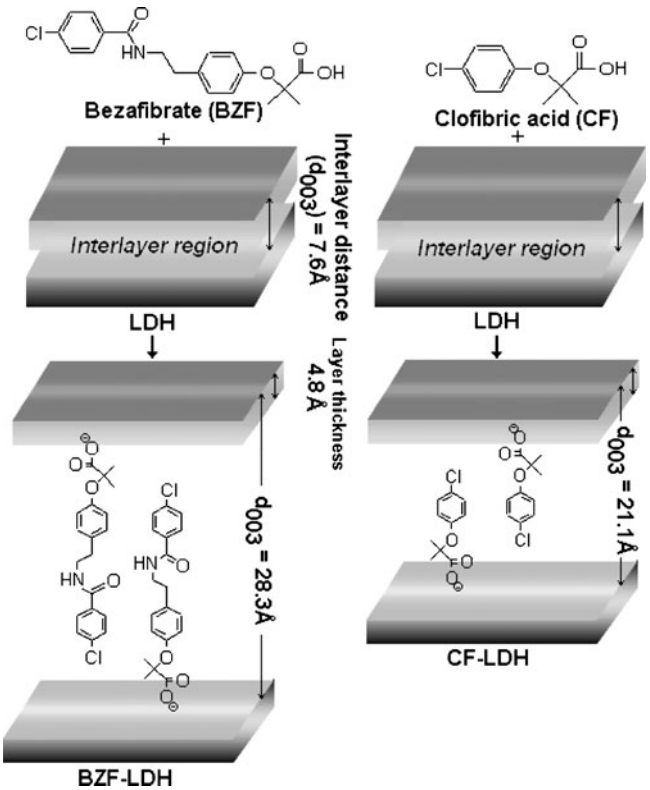

Fig. 2 Systematic diagram of drug-LDH intercalation process.

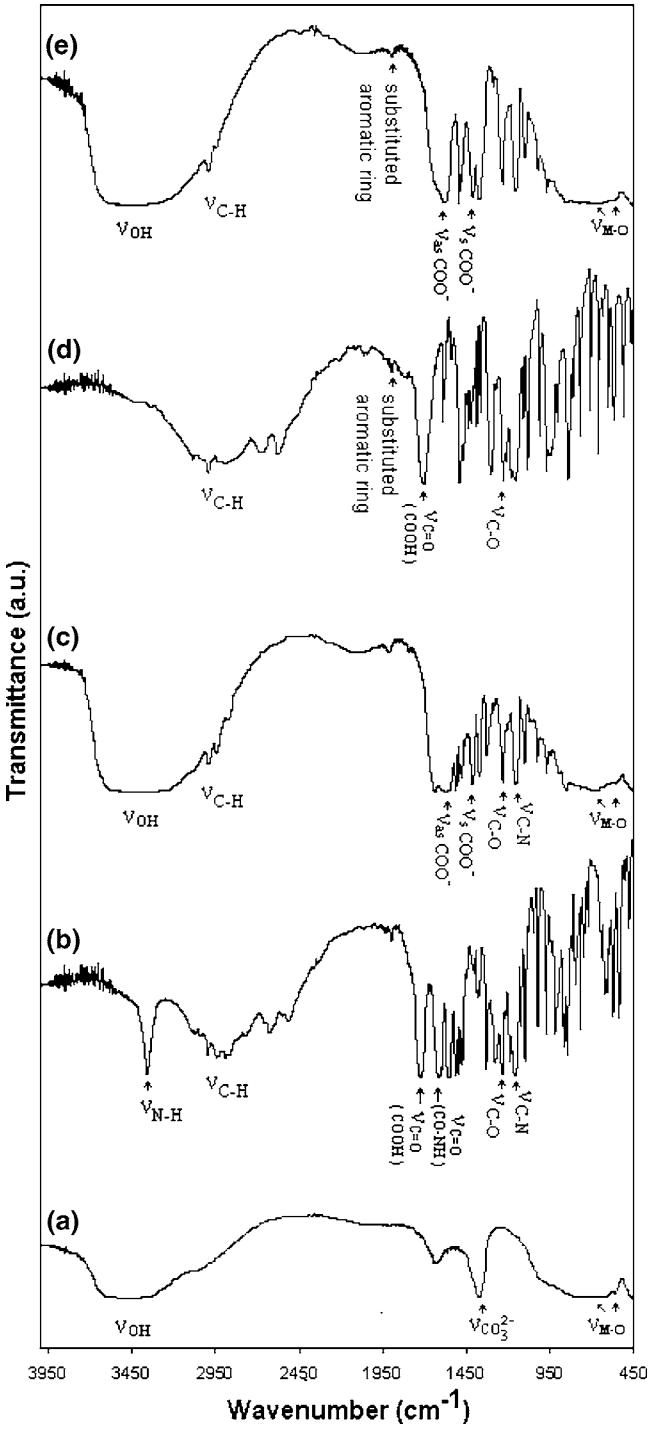

Fig. 3 Infrared spectra of LDH (**a**), BZF (**b**), BZF-LDH (**c**), CF (**d**) and CF-LDH (**e**).

spacing was calculated to be 7.6Å. As a result of intercalation, the reflections (*00 l*) shifted to lower angles with an increase in the basal spacing (28.3Å for BZF-LDH and 21.1Å for CF-LDH, respectively). The strong and symmetrical diffraction peaks reflected a good crystallinity for the obtained nanocomposites. The absence of original LDH peaks indicated a successful synthesis of nanocomposites with single phase incorporation of BZF and CF (patterns b and c, respectively). The interlayer distance of nanocomposite was calculated by subtracting the inorganic layer thickness (4.8Å) (23) from the *d003*-spacing. The determined values were 23.5 and 16.3Å for BZF-LDH and CF-LDH, respectively. These values were larger than drugs molecular lengths (18.1Å for BZF and 10.9Å for CF). Thus, we speculated that the drugs were stacked as a monolayer

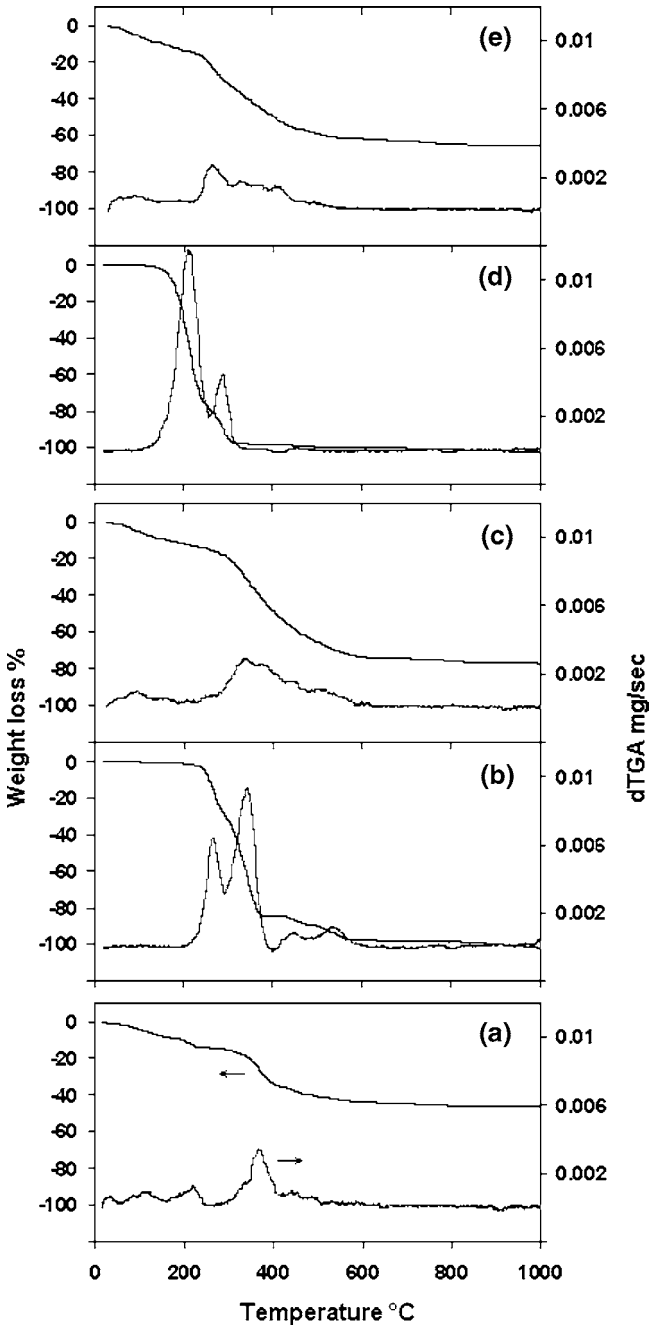

Fig. 4 Thermogravimetric analysis and their differential curves of LDH (**a**), BZF (**b**), BZF-LDH (**c**), CF (**d**) and CF-LDH (**e**).

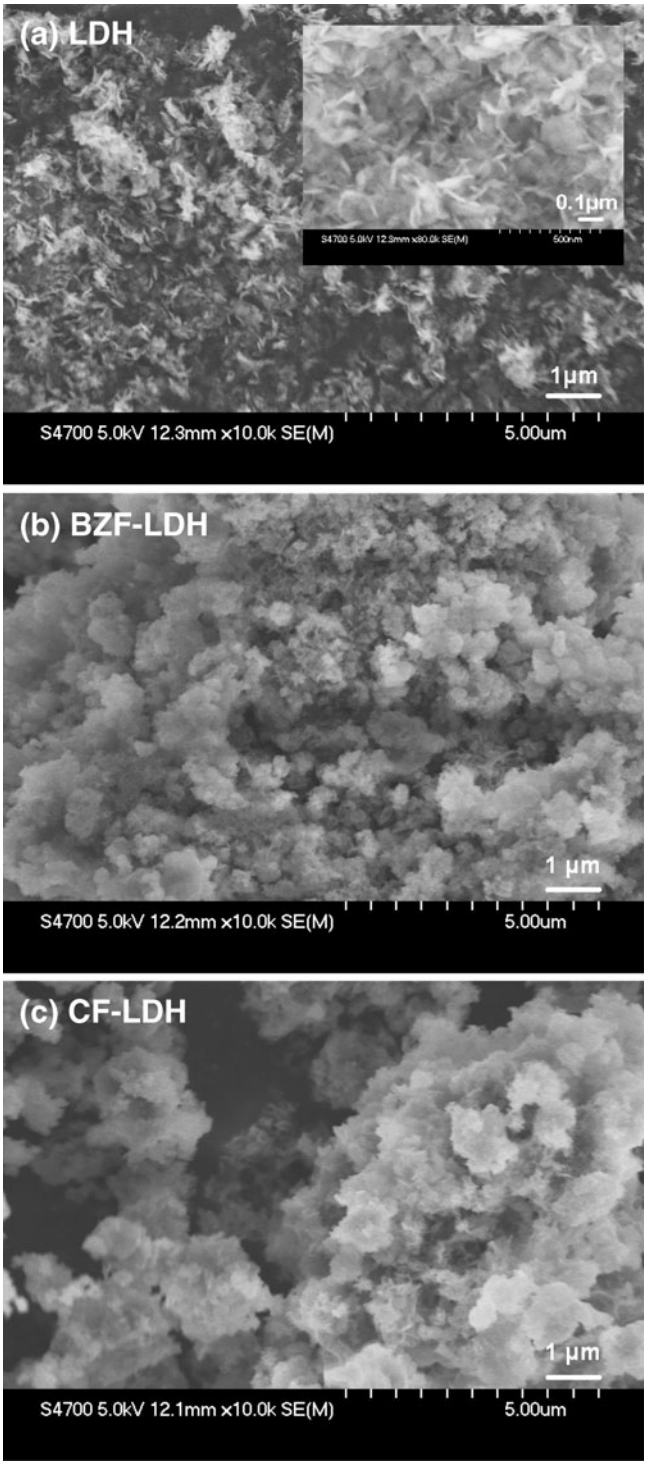

Fig. 5 SEM images of LDH (**a**), BZF-LDH (**b**) and CF-LDH (**c**).

in a staggered inter-digitated arrangement through aromatic rings' π-π interaction as we schematically drew in Fig. 2. The weaker diffraction intensities of CF-LDH (Fig. 1c) than BZF-LDH (Fig. 1b) probably resulted from the small number of aromatic rings in CF molecules.

Infrared Spectroscopy

FT-IR spectra were measured to obtain further information about the nanocomposites' molecular structure. Figure 3a shows the characteristic peaks of LDH, the asymmetric stretching band of the interlayer carbonate group ($\nu_{CO_3^{2-}}$) and the hydroxyl group's stretching vibration band (ν_{OH}) of LDH layers were observed at 1379 and 3450 cm^{-1}, respectively (24). The lattice vibration modes of the layers (ν_{M-O}) were detected at 711 and 574 cm^{-1} (25). In Fig. 3b (BZF powder), the bands of ν_{C-N}, ν_{C-O}, and ν_{N-H} were detected at 1153, 1232, and 3365 cm^{-1}, respectively. The stretching vibration band $\nu_{C=O}$ of the amide group and that of COOH group were detected at 1620 and 1732 cm^{-1}, respectively. The weak stretching vibration modes ν_{C-H} of

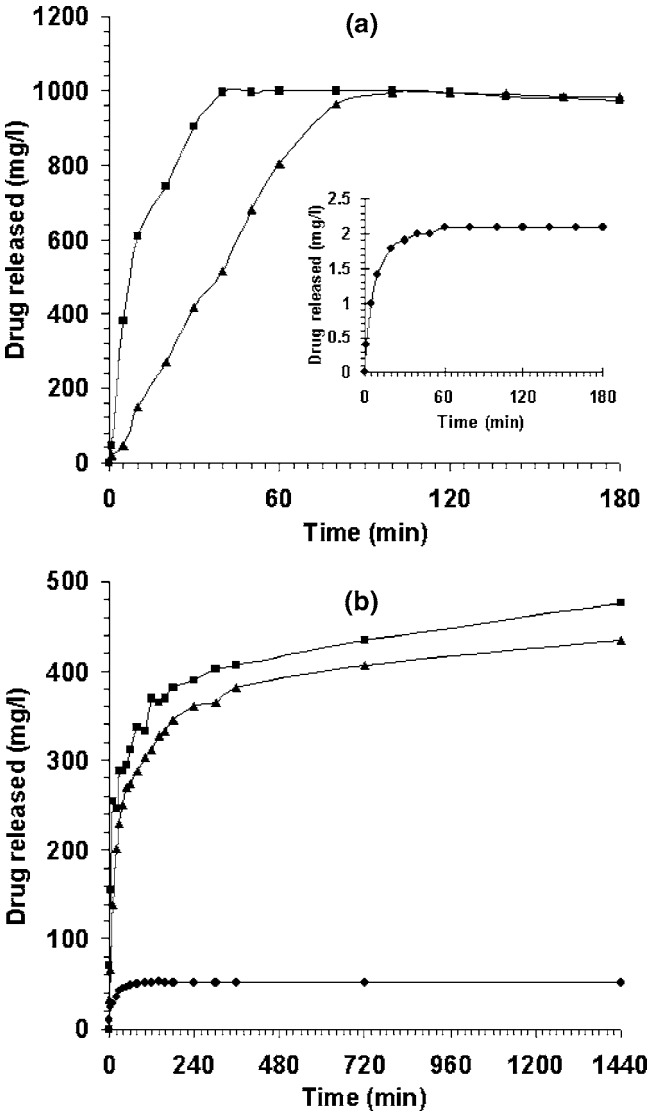

Fig. 6 Drug release of BZF in buffer A (♦), buffer B (▲) and buffer C (■): before intercalation (**a**) and after intercalation (**b**).

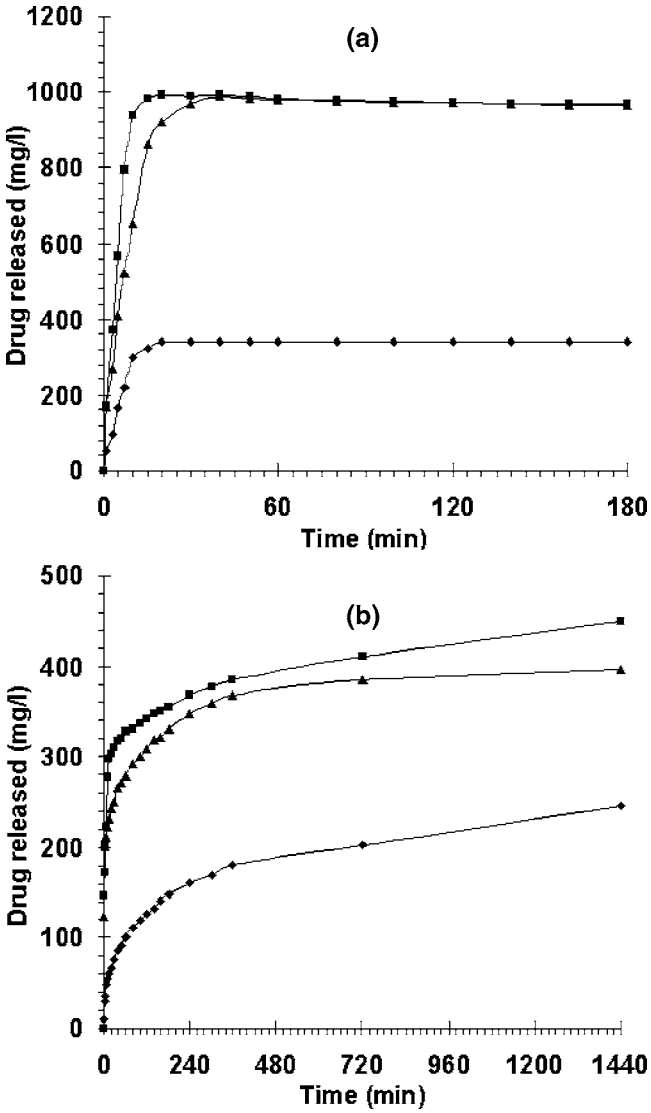

Fig. 7 Drug release of CF in buffer A (♦), buffer B (▲) and buffer C (■): before intercalation (**a**) and after intercalation (**b**).

BZF alkyl groups were detected between 3000 and 2900 cm^{-1}. As a result of intercalation of BZF into LDH (Fig. 3c), new peaks were detected such as symmetric and asymmetric modes of COO^{-} at 1411 and 1604 cm^{-1}, respectively, beside the characteristic peaks of BZF and LDH. This information indicated that BZF molecules combined with LDH layers through electrostatic interaction. The complete disappearance of carbonate group in BZF-LDH spectrum confirmed the formation of LDH nanocomposites with single phase incorporation of BZF. Similar changes in FT-IR spectrum of CF-LDH (*i.e.*, the complete disappearance of v_{CO3}^{2-} and the emergence of symmetric and asymmetric bands of COO^{-} group) were observed (Fig. 3e). These changes confirmed the formation of CF-LDH nanocomposite with single phase incorporation of CF.

Thermal Analysis

Figure 4 displays the TGA curves of the prepared samples and the pure drugs. In the case of original LDH (Fig. 4a), the weight loss was observed to proceed in three steps: 90–150°C (8 % loss, loss of physically adsorbed water), 170–260°C (7% loss, loss of interlayer water), and 250–510°C (30% loss, hydroxylation and carbonate decomposition) (26,27). The TGA curve significantly changed in the case of nanocomposites. The amount of interlayer water decreased to 4% for BZF-LDH and 3% for CF-LDH probably due to the hydrophobic nature of the intercalated drugs. The overall weight loss increased to 75% and 66% for BZF-LDH (Fig. 4c) and CF-LDH (Fig. 4e), respectively. The higher weight loss in BZF-LDH than CF-LDH indicates the higher BZF weight content in its LDH nanocomposites. The drug-LDH nanocomposites showed an improved stability against thermal decomposition after the intercalation process. Especially in CF-LDH, the onset temperature of decomposition shifted considerably, from 100°C of original CF to 220°C. Accordingly, LDH nanocomposites supported the safe preservation of BZF and CF drugs.

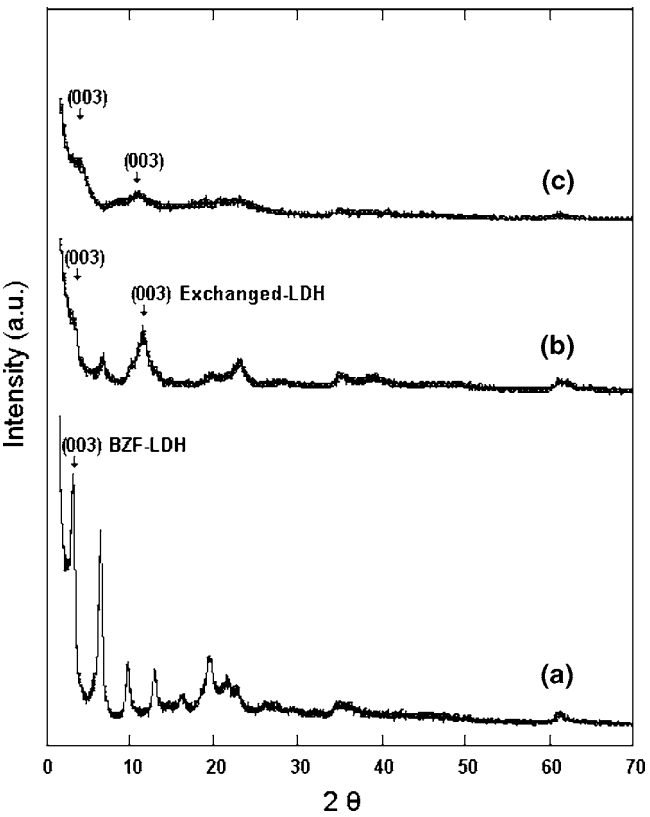

Fig. 8 X-ray diffraction patterns of BZF-LDH: before release (**a**), the residual of the releasing medium of buffer A (**b**), and the residual of the releasing medium of buffer C (**c**).

SEM Observation

The SEM images of original LDH and nanocomposites are shown in Fig. 5. Original LDH (image a) shows regular hexagonal platelet structure. This regularity indicated the good crystallinity determined by X-ray measurement. In the case of BZF-LDH and CF-LDH nanocomposite (images b and c), such regular structure was decreased, and aggregates composed of small particles (diameter~ 0.1 μm) were observed. The large surface area resulting from nanocomposite's small particle size is expected to improve the drug's solubility and dissolution rate.

Drug Delivery and Dissolution from Nanocomposites

The weight contents of BZF and CF in their nanocomposites were determined to be 54% and 45%, respectively. The higher content in BZF-LDH agreed with the result of TGA. Figure 6a shows the solubility of BZF drug powder at the different mediums. The solubility was very small in buffer A, due to the acidic character of BZF. The drug was completely dissolved after 80 min (buffer B) and 40 min (buffer C), due to deprotonation of carboxylic acid group at high $pH_{(s)}$. Such release data indicates the uncontrollable dissolution of BZF in the alkaline small intestine after the burst of the drug-capsule prepared by the previously mentioned conventional methods. Figure 6b shows the release of BZF from the nanocomposite. Significant change in the amount of BZF released was observed with time progress. Around 40% and 45% was released during 24 h in buffer B and C, respectively, while only 5% was obtained in buffer A at the same time. The release of BZF depended on medium anionic species and LDH nanocomposite properties. However, LDH possesses an anion exchange selectivity for carbonate than chloride (28–30), the release of BZF in buffers B and C was higher than buffer A. On the other side, the layered molecular structure of LDH has limited the interaction of BZF in two-dimensional directions. This stacking process has prevented the crystallization of BZF into LDH layers, and accordingly the drug was released in its amorphous form. The anion exchange mechanism of LDH (30) has controlled the release of BZF from the nanocomposites. The phase boundary formed between the internal zone (drug-LDH, large d-spacing) and the external zone (exchanged LDH, small spacing) during the anion exchange process has decreased the amount of drug released with time progress.

The release studies of CF (Fig. 7) showed similar behaviors and changes as BZF did before and after nanocomposite formation. The differences were observed only in amounts and release times of CF. The improved release properties of CF-LDH were also related to medium anionic species and LDH nanocomposite properties. At this stage and from the release data of BZF-LDH and CF-LDH, we can say that nanocomposite formulation with LDH supported the delivery and the controlled release properties of the studied lipid-regulating drugs.

Drug Release Mechanism

To confirm the replacement of drug molecule with the buffer anionic species, XRD measurement was performed after the dissolution experiment of BZF-LDH (Fig. 8). Patterns b and c showed new reflection peaks at high 2θ beside the original BZF-LDH reflections. The calculated d-spacing of the new reflections was found to be 7.8 and 7.65Å for patterns b and c, respectively. These new d-spacing values indicated the anion exchange of BZF with chloride and carbonate anions, respectively (28). The higher broadness and the poorer crystallinity of pattern c than pattern b reflected the high disorder of LDH layers resulting from the high exchange process; similar behavior was noticed by Chitrakar *et al.* (31) through the exchange of phosphate.

CONCLUSION

Nanocomposites composed of fibrate derivatives (BZF and CF) with LDH were successfully synthesized by co-precipitation technique. X-ray measurement and spectroscopic analysis indicated the formation of fully monophase nanoparticles. The LDH nanocomposite formulation system has improved the selected drugs properties (thermal stability, dissolution, controlled release and target delivery).

ACKNOWLEDGMENTS

This work was partly supported by the Feasibility Study grant from JST Innovation Satellite Tokushima, Japan.

REFERENCES

1. Craig WY, Palomaki GE, Haddow JE. Cigarette smoking and serum lipid and lipoprotein concentrations: an analysis of published data. Br Med J. 1989;298:784–8.
2. Ordovas JM. The genetics of serum lipid responsiveness to dietary interventions. Proc Nutr Soc. 1999;58:171–87.
3. Remick J, Weintraub H, Setton R, Offenbacher J, Fisher E, Schwartzbard A. Fibrate therapy: an update. Card Rev. 2008;16:129–41.
4. Ayaori M, Momiyama Y, Fayad ZA, Yonemura A, Ohmori R, Kihara T, *et al.* Effect of bezafibrate therapy on atherosclerotic aortic plaques detected by MRI in dyslipidemic patients with hypertriglyceridemia. Atherosclerosis. 2008;196:425–33.
5. Emblidge JP, DeLorenzo ME. Preliminary risk assessment of the lipid-regulating pharmaceutical clofibric acid, for three estuarine species. Environ Res. 2006;100:216–26.

6. Miller DB, Spence JD. Clinical pharmacokinetic of fibric acid derivatives (fibrates). Clin Pharmacokinet. 1998;34(2):155–62.
7. Winkler M, Lawrence JR, Neu TR. Selective degradation of ibuprofen and clofibric acid in two model river biofilm systems. Water Res. 2001;35:3197–205.
8. Rajeev AJ, Luis B, Julie AS, Todd T, Howard B. Effect of powder processing on performance of fenofibrate formulations. Eur J Pharm Biopharm. 2008;69:727–34.
9. Markus V, Klaus K, Jennifer BD. Dissolution enhancement of fenofibrate by micronization, cogrinding and spray-drying: Comparison with commercial preparations. Eur J Pharm Biopharm. 2008;68:283–8.
10. Pol-Henri G, Michael GV, Diana F. A new fenofibrate formulation: Results of six single-dose, clinical studies of bioavailability under fed and fasting conditions. Clin Ther. 2004;26:1456–69.
11. Costantino U, Marmottini F, Nocchetti M, Vivani R. New synthetic routes to hydrotalcite-like compounds: characterisation and properties of the obtained materials. Eur. J. Inorg. Chem. 1439–1446 (1998).
12. Ogawa M, Kaiho H. Homogeneous precipitation of uniform hydrotalcite particles. Langmuir. 2002;18:4240–2.
13. Darder M, Blanco ML, Aranda P, Leroux F, Hitzky ER. Bionanocomposites based on layered double hydroxides. Chem Mater. 2005;17:1969–77.
14. Li B, He J, Evans DG, Duan X. Enteric-coated layered double hydroxides as a controlled release drug delivery system. Int J Pharm. 2004;287:89–95.
15. Tronto J, Reis MJ, Silvério F, Balbo VR, Marchetti JM, Valim JB. *In vitro* release of citrate anions intercalated in magnesium aluminum layered double hydroxides. J Phys Chem. 2004;65:475–80.
16. Bingxin L, Jing H, Evans DG, Xue D. Inorganic layered double hydroxides as a drug delivery system: intercalation and *in vitro* release of fenbufen. Appl Clay Sci. 2004;27:199–207.
17. Berber MR, Minagawa K, Katoh M, Mori T, Tanaka M. Nanocomposites of 2-arylpropionic acid drugs based on Mg-Al layered double hydroxide for dissolution enchancement. Eur J Pharm Sci. 2008;35:354–60.
18. Aisawa S, Higashiyama N, Takahashi S, Hirahara H, Ikematsu D, Kondo H, *et al.* Intercalation behavior of L-ascorbic acid into layered double hydroxides. Appl Clay Sci. 2007;35:146–54.
19. Sokolova V, Epple M. Inorganic nanoparticles as carriers of nucleic acids into cells. Angew Chem Int Ed. 2008;47:1382–95.
20. Costantino U, Ambrogi V, Nocchetti M, Perioli L. Hydrotalcite-like compounds: Versatile layered hosts of molecular anions with biological activity. Microporous Mesoporous Mat. 2008;107:149–60.
21. White JF. Bicarbonate-dependent chloride absorption in small intestine: Ion fluxes and intracellular chloride activities. J Membrane Biol. 1980;53:95–107.
22. Vatier J, Malikova-Sekera E, Vitre MT, Mignon M. An artificial stomach-duodenum model for the *in-vitro* evaluation of antacids. Aliment Pharmacol Ther. 1992;6:447–58.
23. Miyata S. The syntheses of hydrotalcite-like compounds and their structures and physico-chemical properties-I: The systems Mg^{2+}-Al^{3+}-NO_3^-, Mg^{2+}-Al^{3+}-Cl^-, Mg^{2+}-Al^{3+}-ClO_4^-, Ni^{2+}-Al^{3+}-Cl^- and Zn^{2+}-Al^{3+}-Cl^-. Clays Clay Miner. 1975;23:369–70.
24. Kuila T, Acharya H, Srivastava SK, Bhowmick AK. Synthesis and characterization of ethylene vinyl acetate/Mg–Al layered double hydroxide nanocomposites. J Appl Poly Sci. 2007;104:1845–51.
25. Lin Y, Wang J, Evans DG, Li D. Layered and intercalated hydrotalcite-like materials as thermal stabilizers in PVC resin. J Phys Chem Solids. 2006;67:998–1001.
26. Lopez T, Bosch P, Asomoza M, Gomez R, Ramos E. DTA-TGA and FTIR spectroscopies of sol-gel hydrotalcites: Aluminum source effect on physicochemical properties. Mat Let. 1997;31:311–6.
27. Labajos FM, Rives V, Ulibarri MA. Effect of hydrothermal and thermal treatments on the physicochemical properties of Mg-Al hydrotalcite-like materials. J Mater Sci. 1992;27:1546–52.
28. Miyata S. Anion exchange properties of hydrotalcite-like compounds. Clays Clay Miner. 1983;31:305–11.
29. Wang SL, Liu CH, Wang MK, Chuang YH, Chiang PN. Arsenate adsorption by Mg/Al–NO_3 layered double hydroxides with varying the Mg/Al ratio. Appl Clay Sci. 2009;43:79–85.
30. Kaneyoshi M, Jones W. Exchange of interlayer terephthalate anions from a Mg-Al layered double hydroxide: formation of intermediate interstratified phases. Chem Phys Lett. 1998;296:183–7.
31. Chitrakar R, Tezuka S, Sonoda A, Sakane K, Ooi K, Hirotsu T. A solvent-free synthesis of Zn–Al layered double hydroxides. Chem Let. 2007;36:446–7.